Thermoacoustic effects in supercritical fluids near the critical point: Resonance, piston effect, and acoustic emission and reflection

Akira Onuki
Department of Physics, Kyoto University, Kyoto 606-8502

We present a general theory of thermoacoustic phenomena in supercritical fluids near the critical point in a one-dimensional cell. We take into account the effects of the heat conduction in the boundary walls and the bulk viscosity near the critical point. We introduce a coefficient $Z(\omega)$ characterizing reflection of sound with frequency ω at the boundary. As applications, we examine the acoustic eigenmodes in the cell, the response to time-dependent perturbations, sound emission and reflection at the boundary. Resonance and rapid adiabatic changes are noteworthy. In these processes, the role of the thermal diffusion layers is enhanced near the critical point because of the strong critical divergence of the thermal expansion.

PACS numbers: 05.70.Jk, 64.70.Fx, 62.60.+v, 65.40.De

I. INTRODUCTION

In highly compressible fluids, adiabatic changes take place with propagation of sounds and are much faster than the thermal diffusion [1]. When a one-component fluid is heated or cooled at a boundary, a thermal diffusion layer expands or shrinks to emit sounds, which then cause adiabatic changes in the interior (the thermal piston effect). The density change in the boundary layer is enhanced near the gas-liquid critical point because of the strong critical growth of the isobaric thermal expansion. As a result, thermal equilibration times become shorter near the critical point at fixed volume, despite the fact that the thermal diffusion constant D tends to zero at the criticality [2, 3, 4, 5, 6, 7, 8, 9, 10, 11]. If the boundary temperature is slightly changed, temperature homogenization occurs throughout the cell on a scale of the piston time [3],

$$t_1 = L^2/4(\gamma-1)^2 D, \tag{1.1}$$

where L is the cell length, D is the thermal diffusion constant, and $\gamma = C_p/C_V$ is the specific-heat ratio growing near the critical point. See Appendix A for a derivation of Eq.(1.1). The time t_1 is much shorter than the isobaric equilibration time $L^2/4D$ by the factor $(\gamma-1)^{-2} \ll 1$. For example, we have $t_1 = 6.3\times 10^4 \epsilon^{1.65}$sec for CO_2 with $L = 1$cm. Hereafter, $\epsilon = T/T_c - 1$ is the reduced temperature near the critical point. The early experiments detected slow temperature and density changes in the interior on time scales much longer than the acoustic time L/c. The fast acoustic processes were examined by numerical simulations of the hydrodynamic equations of compressible fluids [6, 12, 13].

Ferrell and Hao [14] found relevance of the heat conduction in the boundary walls in transient heat transport. That is, the thermal boundary condition of a cell containing a near-critical fluid crosses over from the isothermal to insulating one even for a metal boundary wall due to the critical divergence of the effusivity of the fluid [15]. The formula (1.1) should then be modified, because it is based on the isothermal boundary condition. More recently, Carlès and Dadzie [16, 17] found that the bulk viscosity, which grows strongly near the critical point, can affect the hydrodynamics in the thermal diffusion layer. Gillis *et al.* [18] performed experiments of acoustic resonance in xenon, where the frequency and attenuation of the resonating modes were measured. For such long wavelength sounds, the heat conduction at the boundary is the dominant damping mechanism relatively far from the critical point, while the viscous effect in the bulk becomes more important closer to the critical point. They also presented thorough theoretical analysis of their data. The critical growth of the effusivity and the bulk viscosity of the fluid both serve to suppress the boundary damping, as confirmed experimentally and theoretically. Very recently, Miura *et al.* [19, 20] measured acoustic density changes with precision of order 10^{-7}g/cm^3 in near-critical CO_2 on the acoustic time scale using a ultra-sensitive interferometer. They detected emission and traversal of sound pulses with width of order 10μsec, which were broadened as they moved through the cell and interacted with the boundary walls. Some of their data agreed with predictions, but most data remain unexplained. Afterwords, part of the measured time-evolution of the density was numerically reproduced by Carlès, neglecting the bulk viscosity [21].

Some unique aspects of the supercritical hydrodynamics have been revealed by experiments [22, 23, 24] and by simulations [13, 25, 26, 27, 28, 29]. In Rayleigh-Bénard convection, overall temperature changes are induced by plume arrivals at the boundary walls due to the piston effect, leading to overshoot behavior observed in experiments of ^{3}He near its critical point [22, 26, 27]. Significant noises of the adiabatic temperature changes were predicted in turbulent convective states [26], though not yet measured systematically. Recently three-dimensional simulations were performed [29]. Due to large thermal expansion in supercritical fluids, jet-like fluid flow has been observed around a heated boundary [23, 24]. In these processes, the plume motions governed by the shear viscosity are strongly influenced by large thermal expansion around a heater and by rapid adiabatic density and

temperature changes achieved by sound propagation.

In this paper, we aim to give detailed analysis of the linear hydrodynamics of supercritical fluids near the critical point in a one-dimensional cell. We take into account the effects of the decreasing effusivity ratio [15] and the growing bulk viscosity. In Section II, we will decompose fluid motions into sound modes and thermal diffusion modes with frequency ω. These two modes are mixed at the boundary under given boundary conditions, leading to various thermoacoustic phenomena. In Section III, we will study the acoustic eigenmodes determined to confirm the calculations by Gillis *et al.*[18] in the simpler one-dimensional geometry. We will also examine the response of the fluid to various time-dependent perturbations. Resonance is induced when the frequency of the perturbation is close to one of the eigenfrequencies, while nearly uniform adiabatic changes are caused in the interior due to the piston effect at much lower frequencies. We will also examine sound emission and reflection at the boundary. In Appendix A, we will present a simple theory of the piston effect, which can be a starting point to understand the complicated calculations in the text. In Appendix B, the critical behavior of one-component fluids used in the text will be summarized.

II. THEORETICAL BACKGROUND

A. Linear hydrodynamics

Near the critical point, we treat the hydrodynamic deviations with spatial scales much exceeding the thermal correlation length ξ, but the typical frequency ω can be higher than the relaxation rate of the critical fluctuations $t_\xi^{-1} \propto \epsilon^{1.89}$ [30]. For such high frequencies ω, the bulk viscosity ζ behaves as $1/\omega$, while $\zeta \propto \epsilon^{-1.67}$ for $\omega t_\xi < 1$ [31, 32, 33]. See Appendix B for more details. The other transport coefficients may be treated to be independent of ω [1]. The critical singularity of the shear viscosity η is negligible small, while the critical growth of the thermal conductivity λ arises from the convective motions of the critical fluctuations taking place on a short time scale of order $\rho\xi^2/\eta$. Here we assume $\omega \ll \eta/\rho\xi^2$.

The mass density, the temperature, the entropy (per unit mass), and the pressure are written as ρ, T, s, and p, respectively, with their small deviations being $\delta\rho$, δT, δs, and δp. The velocity in the x direction is written as v. These deviations depend on time t as $\exp(i\omega t)$ and vary in space along the x axis. We may assume $\omega > 0$ without loss of generality (see Eq.(3.1)). These deviations may be regarded as the Fourier transformations of the space-time dependent deviations with respect to time $(= \int dt e^{-i\omega t}(\cdots))$. They obey the linear equations [34],

$$i\omega\delta\rho = -\rho v', \tag{2.1}$$
$$i\omega\rho v = -\delta p' + \rho\nu_\ell v'', \tag{2.2}$$
$$i\omega\rho T\delta s = \lambda\delta T''. \tag{2.3}$$

Here the prime denotes the differentiation with respect to x. We have two dissipative coefficients; one is the thermal conductivity λ and the other is

$$\nu_\ell = (\zeta + 4\eta/3)/\rho, \tag{2.4}$$

where ζ and η are the bulk and shear viscosities, respectively. Using the thermodynamic derivatives we may express δs and δp in terms of $\delta\rho$ and δT as

$$\rho T\delta s = C_V[\delta T - b_s^{-1}\delta\rho], \tag{2.5}$$
$$\delta p = \gamma^{-1}c^2\delta\rho + (1-\gamma^{-1})a_s\delta T, \tag{2.6}$$

where $c^2 = (\partial p/\partial\rho)_s$ is the square of the sound velocity,

$$\gamma = C_p/C_V \tag{2.7}$$

is the specific-heat ratio with $C_p = \rho T(\partial s/\partial T)_p$ and $C_V = \rho T(\partial s/\partial T)_\rho$ being the isobaric and constant-volume specific heat (per unit volume), respectively. To avoid cumbersome notation, we write

$$a_s = \left(\frac{\partial p}{\partial T}\right)_s, \quad b_s = \left(\frac{\partial \rho}{\partial T}\right)_s = c^{-2}a_s. \tag{2.8}$$

For low-frequency sounds, the adiabatic relations $\delta p \cong a_s\delta T$ and $\delta\rho \cong b_s\delta T$ should hold. We use the following thermodynamic identities [1],

$$\left(\frac{\partial p}{\partial T}\right)_\rho = (1-\gamma^{-1})a_s = \rho c^2 C_V/Ta_s. \tag{2.9}$$

Next we consider small hydrodynamic deviations by assuming the space-dependence in the sinusoidal form $\exp(iqx)$. From Eqs.(2.3) and (2.5) $\delta\rho$ and δT are related by

$$\delta T = \frac{i\omega c^2}{(i\omega + \gamma Dq^2)a_s}\delta\rho, \tag{2.10}$$

where $D = \lambda/C_p$ is the thermal diffusion constant. Equations Eq.(2.1)-(2.3) give the dispersion equation between q and ω,

$$[\omega^2 - (i\omega\nu_\ell + \gamma^{-1}c^2)q^2](i\omega + \gamma Dq^2) = i\omega c^2(1-\gamma^{-1})q^2. \tag{2.11}$$

If we set $q = \omega/c\sqrt{X}$ or $X = (\omega/cq)^2$, the dimensionless quantity X obeys the quadratic equation,

$$X^2 - (1 + \Delta_v + \gamma\Delta_T)X + (1+\gamma\Delta_v)\Delta_T = 0. \tag{2.12}$$

where we introduce two dimensionless coefficients representing the dissipation strength [18],

$$\Delta_v = i\omega\nu_\ell/c^2, \tag{2.13}$$
$$\Delta_T = i\omega D/c^2. \tag{2.14}$$

If $\omega > 0$, Δ_v and Δ_T are purely imaginary. The ratio $\Delta_v/\Delta_T = \nu_\ell/D$ grow strongly near the critical point (see Appendix B).

For given ω, Eq.(2.11) or Eq.(2.12) yields four solutions $q = \pm q_\pm = \pm\omega/c\sqrt{X_\pm}$, where X_+ and X_- are the solutions of Eq.(2.12) written as [18]

$$\begin{aligned} X_\pm &= \frac{1}{2}(1+\Delta_v+\gamma\Delta_T \mp \Xi), \\ &= \frac{2(1+\gamma\Delta_v)\Delta_T}{1+\Delta_v+\gamma\Delta_T \pm \Xi}, \end{aligned} \tag{2.15}$$

where we define

$$\Xi = [(1+\Delta_v-\gamma\Delta_T)^2 + 4(\gamma-1)\Delta_T]^{1/2}, \tag{2.16}$$

with $\mathrm{Re}\Xi > 0$. The second line of Eq.(2.15) follows from $X_+X_- = (1+\gamma\Delta_v)\Delta_T$. The modes with $q = \pm q_-$ represent the sound, while those with $q = \pm q_+$ the thermal diffusion. We may define q_- and q_+ such that $\mathrm{Re}(q_-/\omega) > 0$ and $\mathrm{Im}q_+ < 0$ hold. It is convenient to introduce k and κ by

$$k = q_- = \frac{\omega}{c\sqrt{X_-}}, \quad \kappa = iq_+ = \frac{i\omega}{c\sqrt{X_+}}. \tag{2.17}$$

The argument of X_- is in the range $[0, \pi/2]$ for $\omega > 0$, leading to $\mathrm{Im}k < 0$, which implies that sound waves propagating in the positive x direction ($\propto e^{-ikx}$) are damped with increasing x.

As $\omega \to 0$, we may treat Δ_v and Δ_T as small quantities. To their first order we find $X_+ \cong \Delta_T$ and $X_- \cong 1+\Delta_v+(\gamma-1)\Delta_T$ so that $\kappa \cong \sqrt{i\omega/D}$ and $k \cong \omega/c - i\Gamma_s\omega^2/2c^3$, where [34]

$$\Gamma_s = (\zeta + 4\eta/3)/\rho + (\gamma-1)D \tag{2.18}$$

is the attenuation constant in the long wavelength limit. We have $|\kappa| \gg |k|$ at low frequencies. For example, $|\kappa| \sim 10^5$ cm^{-1} and $|k| \sim 10^{-2}$ cm^{-1} for $\omega = 10^4$ s^{-1}, $D = 10^{-6}$ cm^{2}s^{-1}, and $c = 10^4$ cm/s. In a cell with length L, the strength of the bulk dissipation of sounds is represented by the damping factor $\exp(-\delta_B L)$ with

$$\begin{aligned} \delta_B &= -\mathrm{Im}k \\ &\cong \Gamma_s\omega^2/2\rho c^3, \end{aligned} \tag{2.19}$$

where the second line is the low-frequency expression. Mathematically, we may consider the high frequency limit $|\Delta_v| \gg 1$ and $|\Delta_T| \gg 1$ neglecting the frequency-dependence of the transport coefficients to derive the limiting behavior $k \to (i\omega/\nu_\ell)^{1/2}$ and $\kappa \to (i\omega/\gamma D)^{1/2}$, though this limit is unrealistic. In this paper, we will assume $|\Delta_T| \ll \gamma^{-1}$ in Eq.(2.34), because it is satisfied in realistic experimental conditions, as will be discussed.

B. Solutions in a finite cell

We consider small hydrodynamic perturbations behaving as $e^{\omega t}$ in a fluid in a finite cell with length L. The density deviation can be expressed in the following linear combination,

$$\delta\rho = ae^{-\kappa x} + be^{\kappa(x-L)} + \alpha e^{ikx} + \beta e^{-ikx}. \tag{2.20}$$

The coefficients a, b, α, and β depend on time as $e^{i\omega t}$. The first and second terms represent the deviations in the thermal diffusion layers. The thickness of the layers is given by $1/|\kappa|$, which is assumed to be much shorter than the cell length L, so

$$|\kappa| \gg 1/L. \tag{2.21}$$

Then the second (first) term is virtually zero near $x = 0$ ($x = L$). The third term in Eq.(2.20) represents a sound propagating in the negative x direction , while the fourth term a sound propagating in the positive x direction. From Eq.(2.1) the velocity is expressed as

$$v = \frac{i\omega}{\rho\kappa}[ae^{-\kappa x} - be^{\kappa(x-L)}] - \frac{\omega}{\rho k}[\alpha e^{ikx} - \beta e^{-ikx}]. \tag{2.22}$$

If the boundary walls are fixed in time, we should require $v = 0$ at $x = 0$ and L to obtain

$$a = (\kappa/ik)(\alpha - \beta), \tag{2.23}$$

$$b = -(\kappa/ik)(\alpha e^{ikL} - \beta e^{-ikL}) \tag{2.24}$$

Note that the mass change in the thermal diffusion layers is $(a+b)/\kappa$ and that in the interior is $\alpha(e^{ikL}-1)/ik + \beta(1-e^{-ikL})/ik$ per unit area. From Eqs.(2.23) and (2.24) these two changes cancel, ensuring the mass conservation. Use of Eq.(2.10) gives the temperature deviation in the following linear combination,

$$\delta T = \frac{i\omega}{b_s}\left[\frac{ae^{-\kappa x} + be^{\kappa(x-L)}}{i\omega - \gamma D\kappa^2} + \frac{\alpha e^{ikx} + \beta e^{-ikx}}{i\omega + \gamma Dk^2}\right]. \tag{2.25}$$

Let $\dot{Q}_0$ and $\dot{Q}_L$ be the heat flux $-\lambda\delta T'$ at $x = 0$ and L, respectively. Use of Eqs.(2.23)-(2.25) gives

$$\frac{\beta-\alpha}{\dot{Q}_0} = \frac{\beta - \alpha e^{2ikL}}{e^{ikL}\dot{Q}_L} = \frac{b_s(\gamma-1)}{\lambda(1+\gamma\Delta_v)}\frac{ik}{k^2+\kappa^2}, \tag{2.26}$$

where $b_s(\gamma-1)/\lambda = \rho/Ta_sD$ with the aid of Eq.(2.9). The above quantities tend to the constant ρ/Ta_sc in the low frequency limit. We may use Eq.(2.26) when $\dot{Q}_0$ is a control parameter or when $\dot{Q}_L$ is measurable.

The coefficients a, b, α, and β can be determined if we specify the boundary conditions at $x = 0$ and L. Hereafter we assume no temperature discontinuity at the boundaries. In most theoretical calculations the boundary temperatures are fixed, but in some papers the bottom heat flux Q_0 is fixed [26]. In this paper, we consider a more realistic boundary condition of the temperature accounting for the thermal conduction in the boundary wall regions [14, 18]. Here we assume that δT tends to zero in the solid far from the boundaries without heat input. In the solid region ($x < 0$), the temperature deviation then decays as $\delta T(0)e^{\kappa_w x}$ with

$$\kappa_w = (i\omega C_w/\lambda_w)^{1/2}, \tag{2.27}$$

where λ_w and C_w are the thermal conductivity and the heat capacity (per unit volume) of the solid, respectively. The $1/|\kappa_w|$ is the thickness of the thermal diffusion layer in the solid and is assumed to be shorter than the thickness of the wall. Without temperature discontinuity at the boundary, the energy balance at $x = 0$ yields

$$\begin{aligned}\delta T' &= \lambda_w \kappa_w \delta T/\lambda \\ &= a_w (i\omega/D)^{1/2} \delta T, \end{aligned} \tag{2.28}$$

where δT and $\delta T'$ are the values at $x = 0$. In the second line, the coefficient a_w is the effusivity ratio [15, 18],

$$a_w = (C_w \lambda_w / C_p \lambda)^{1/2}. \tag{2.29}$$

For CO_2 in a Cu cell [20] we have $a_w = 3 \times 10^3 \epsilon^{0.92}$. The boundary temperature at $x = 0$ is fixed or $\delta T(0) = 0$ for $a_w \to \infty$, while the boundary is thermally insulating or $(d\delta T/dx)_{x=0} = 0$ as $a_w \to 0$. On the other hand, if the other boundary wall in the region $x > L$ is made of the same material, the boundary condition at $x = L$ reads

$$\delta T' = -a_w (i\omega/D)^{1/2} \delta T, \tag{2.30}$$

with the same a_w as in Eq.(2.28), where δT and $\delta T'$ are the values at $x = L$.

The boundary conditions at $x = 0$ give Eqs.(2.23) and (2.28), from which we may readily calculate the reflection factor $Z \equiv \beta/\alpha$ between the outgoing and incoming sound waves. It is convenient to introduce the combination,

$$W = \frac{\alpha - \beta}{\alpha + \beta} = \frac{1 - Z}{1 + Z}, \tag{2.31}$$

because W is a small quantity in our system. Some calculations yield a general expression,

$$W = \frac{-ik(i\omega - \gamma D \kappa^2)/\kappa}{i\omega + \gamma D J^2 + \sqrt{i\omega D}(\kappa^2 + k^2)/a_w \kappa}, \tag{2.32}$$

in terms of k and κ. In the case of a thermally insulating boundary, we have $W = 0$ and $Z = 1$ by setting $a_w \to 0$ in Eq.(2.32). The interaction of sounds and the boundary wall is characterized by Z or W, where the wall properties appear only through the effusivity ratio a_w and the system length L does not appear.

C. Adiabatic condition in the interior

We will clarify an upper bound of the frequency, below which the sound motions in the interior are *adiabatic* or without entropy deviations. Under this adiabatic condition, the results from the linear hydrodynamic equations can be much simplified.

Far from the boundary walls or outside the thermal diffusion layers, we may neglect the localized modes to obtain the interior hydrodynamic deviations. From Eqs.(2.5), (2.6), and (2.25), those of the density, temperature, and pressure are related by

$$\begin{aligned}\delta\rho &= [1 + \gamma D k^2/i\omega] b_s \delta T, \\ \delta p &= [1 + D k^2/i\omega] a_s \delta T. \end{aligned} \tag{2.33}$$

Here x and $L - x$ are much longer than $1/|\kappa|$. The second terms in the brackets arise from a small entropy deviation in the interior. Since $\gamma > 1$, the usual adiabatic relations hold in the interior under the condition,

$$|\gamma D k^2/i\omega| \sim \gamma |\Delta_T| \ll 1 \quad \text{or} \quad \omega \ll c^2/\gamma D, \tag{2.34}$$

where Δ_T is defined by Eq.(2.14). This condition is well satisfied in the usual hydrodynamic processes. Even near the critical point, the time $t_{ad} \equiv \gamma D/c^2$ remains very short. For example, $t_{ad} = 7.6 \times 10^{-14} \epsilon^{-0.62}$sec for CO_2.

Under Eq.(2.34) we have $\Xi \cong 1 + \Delta_v$ so that X_+ and X_- in Eq.(2.15) are approximated as

$$X_+ = \frac{1 + \gamma \Delta_v}{1 + \Delta_v} \Delta_T, \quad X_- = 1 + \Delta_v. \tag{2.35}$$

The wave numbers k and κ are expressed as

$$\kappa = \left(\frac{i\omega}{D}\right)^{1/2} \left(\frac{1 + \Delta_v}{1 + \gamma \Delta_v}\right)^{1/2}, \quad k = \frac{\omega/c}{\sqrt{1 + \Delta_v}}. \tag{2.36}$$

We retain Δ_v, since it becomes appreciable near the critical point because of the strong critical divergence of ζ. As will be discussed in Appendix B, $\zeta \cong \rho c^2 R_B t_\xi$ for $\omega t_\xi < 1$, where $R_B \cong 0.03$ is a universal number and $t_\xi = \xi^2/D$ is the characteristic time of the critical fluctuations with ξ being the correlation length. Carlès found the dependence of κ on the singular combination $\gamma\zeta$ as in Eq.(2.36) [16, 17]. By setting $\gamma \Delta_v = i\omega t_B$, we introduce a new characteristic time t_B as

$$t_B = \gamma \zeta/\rho c^2 = R_B \gamma t_\xi. \tag{2.37}$$

Then $t_B \gg t_\xi$ once $R_B \gamma \gg 1$. For CO_2, $t_B = 1.9 \times 10^{-15} \epsilon^{-3.0}$sec. See Table 1 and Fig. 1 for the characteristic times with $L = 1$cm, where t_B exceeds the acoustic time L/c for $\epsilon < 3 \times 10^{-4}$ and the modified piston time t_1' (to be introduced in Eq.(3.16)) for $\epsilon < 3 \times 10^{-5}$. There can be a sizable frequency range with $t_B^{-1} < \omega < t_\xi^{-1}$ at small ϵ, where κ becomes independent of ω as

$$\kappa \cong (\rho c^2/\gamma D \zeta)^{1/2} \cong (R_B \gamma)^{-1/2} \xi^{-1}. \tag{2.38}$$

The thickness of the thermal diffusion layer $1/|\kappa|$ remains longer than ξ by $(R_B \gamma)^{1/2}$. Also from the expression of k in Eq.(2.36) we write the sound dispersion relation as $k = \omega/c^*(\omega)$, where we define the complex sound velocity[1],

$$c^*(\omega) = c\sqrt{1 + \Delta_v}, \tag{2.39}$$

whose critical behavior will be discussed in Appendix B.

As ϵ is decreased, we first encounter the regime where W grows but $a_w \gg 1$ and $\omega t_B \ll 1$ still hold. However,

TABLE I: Parameters of CO_2 in a Cu cell with $L = 1$ cm for $\epsilon = 10^{-3}$ (first line), 10^{-4} (second line), and 10^{-5} (third line). Times are in sec.

γ	a_w	$t_\xi \times 10^6$	$t_B \times 10^6$	$L/c \times 10^4$	$t_1' $	$t_2 \times 10^8$
260	5.0	0.24	1.9	0.71	1.0	0.12
3600	0.63	18	1900	0.83	0.1	1.7
5×10^4	0.075	1300	1.7×10^6	0.98	0.08	3.0

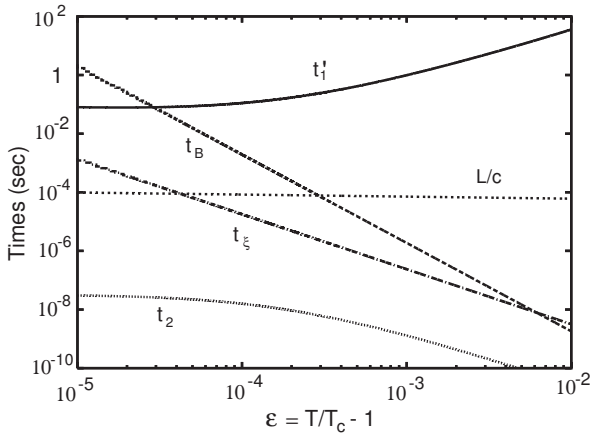

FIG. 1: Characteristic times t_ξ in Eq.(B3), t_B in Eq.(2.37), t_2 in Eq.(2.43), t_1' in Eq.(3.16), and L/c vs $\epsilon = T/T_c - 1$ for CO_2 in a Cu cell with $L = 1$cm.

the critical growth of W is eventually suppressed by the growing a_w^{-1} and ζ. If we use Eqs.(2.35) and (2.36) under Eq.(2.34), we approximate W in Eq.(2.32) as

$$W = \frac{(\gamma-1)\sqrt{\Delta_T}}{(1+\Delta_v)X_v}, \tag{2.40}$$

where we define

$$X_v = \sqrt{1+\gamma\Delta_v} + a_w^{-1}\sqrt{1+\Delta_v}. \tag{2.41}$$

The limiting behaviors of X_v are as follows: $X_v \cong 1+a_w^{-1}$ for $\omega \ll t_B^{-1}$ and $X_v \cong (i\omega t_B)^{1/2}$ for $\omega \gg t_B^{-1}(1+a_w^{-1})^2$.

For $\omega \ll t_B^{-1}$, it follows the classical expression valid far from the critical point,

$$W = (\gamma-1)\sqrt{\Delta_T}/(1+a_w^{-1}) = \sqrt{it_2\omega}, \tag{2.42}$$

which is the result without the viscous effect and under the isothermal boundary condition. We may introduce a characteristic time t_2 defined by

$$t_2 = [a_w/(1+a_w)]^2(\gamma-1)^2 D/c^2, \tag{2.43}$$

which includes the effect of the heat conduction in the wall. As shown in Table 1 and Fig. 1, t_2 is very short even compared with t_ξ. In the literature (see Section 77 of Ref.[34]), it is argued that the amplitude of a plane wave sound is decreased by the factor $(\gamma-1)\sqrt{2D\omega}/c$ upon reflection at an isothermal boundary wall. This factor is obviously equal to $1-|Z| \cong 2\mathrm{Re}W$ if use is made of Eq.(2.42).

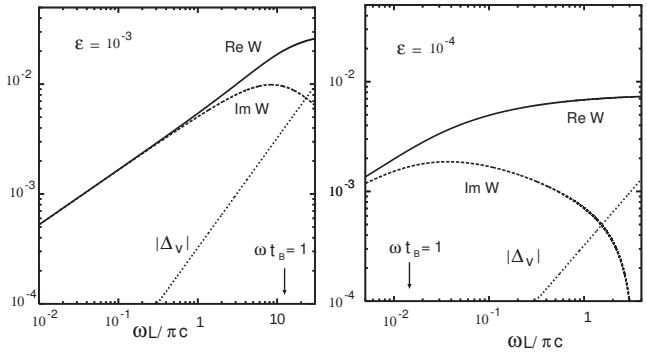

FIG. 2: ReW, ImW, and $|\Delta_v| = \omega\zeta/\rho c^2$ vs $\omega L/\pi c$ at $\epsilon = 10^{-3}$ (left) and 10^{-4} (right) for CO_2 in a Cu cell with $L = 1$cm. As ω exceeds t_B^{-1}, ReW tends to saturate and ImW decreases, due to the growing bulk viscosity and the decreasing effusivity ratio.

In Fig. 2, ReW and ImW are displayed as functions of ω at $\epsilon = 10^{-3}$ and 10^{-4}. While $\omega t_B < 1$, they increase with increasing ω obeying Eq.(2.42). After ω exceeds t_B^{-1}, $\sqrt{1+\gamma\Delta_v}$ becomes $\sqrt{\gamma\Delta_v}$ in Eq.(2.41); then, ReW tends to saturate and ImW decreases. In fact, for $\omega \gg t_B^{-1}(1+a_w^{-1})^2$, we have $X_v \cong \sqrt{\gamma\Delta_v}$ and

$$W \cong (\gamma D/\nu_\ell)^{1/2} \cong W_0\epsilon^{0.64}, \tag{2.44}$$

where $W_0 \cong 2.1$ for CO_2. Also as a function of ϵ, ReW exhibits a maximum around the reduced temperature at which $t_B \sim \omega^{-1}$, as will be shown in Fig. 3. Growing $a_w^{-1}(\propto \epsilon^{-1.14})$ further serves to decrease W. Thus, even close to the critical point, we find $|W| \ll 1$ and

$$Z = 1 - 2W + \cdots. \tag{2.45}$$

D. Hydrodynamic variables in the adiabatic condition

Under Eq.(2.34) we obtain simple expressions of the deviations of the temperature, the pressure, and the entropy including Δ_v. From Eqs.(2.5), (2.6), (2.9), and (2.20) we find

$$\delta T = \left(\frac{\partial T}{\partial \rho}\right)_p (1+\gamma\Delta_v)[\delta\rho]_b + {b_s}^{-1}[\delta\rho]_{in} \tag{2.46}$$

$$\delta s = \left(\frac{\partial s}{\partial \rho}\right)_p (1+\Delta_v)[\delta\rho]_b, \tag{2.47}$$

$$\delta p = -c^2\Delta_v[\delta\rho]_b + c^2[\delta\rho]_{in}, \tag{2.48}$$

where $[\delta\rho]_b = ae^{-\kappa x} + be^{\kappa(x-L)}$ is the density deviation localized near the boundaries and $[\delta\rho]_{in} = \alpha e^{ikx} + \beta e^{-ikx}$ is the interior density deviation. In deriving Eq.(2.46) use has been made of the thermodynamic relation $(1-\gamma)b_s = (\partial\rho/\partial T)_p$. Under Eq.(2.34), the entropy deviation δs is localized near the boundaries, while the localized part of the pressure deviation δp is nonvanishing to satisfy

$i\omega\rho v = -\delta p' + \rho\nu_\ell v'' = -\delta p' - i\omega\nu_\ell\delta\rho' \to 0$ as $x \to 0$ and L in Eq.(2.2).

We examine the deviations close to the boundary at $x = 0$ by asssuming Eqs.(2.23) and (2.28) and setting $Z\alpha = \beta$. In this case the density ratio $[\delta\rho]_b/[\delta\rho]_{in}$ tends to $(\gamma-1)/X_v\sqrt{1+\gamma\Delta_v}$ as $x \to 0$, so that

$$b_s\delta T = (\alpha+\beta)\left[1 - \frac{1}{X_v}\sqrt{1+\gamma\Delta_v}e^{-\kappa x}\right], \quad (2.49)$$

$$\frac{\delta p}{c^2} = (\alpha+\beta)\left[1 - \frac{(\gamma-1)\Delta_v}{X_v\sqrt{1+\gamma\Delta_v}}e^{-\kappa x}\right], \quad (2.50)$$

where $0 < x \ll 1/|k|$. Note that the second terms in the brackets in Eqs.(2.49) and (2.50) tend to unity for $\omega t_B \gg (1+a_w^{-1})^{-2}$, which can be the case of very large ζ. In the original work [3], the pressure homogeneity and the isobaric relations among the hydrodynamic variables were assumed in the thermal diffusion layers. We recognize that the pressure homogeneity and the isobaric condition hold only in the low frequency limit $\omega \ll t_B^{-1}(1+a_w^{-1})^{-2}$.

III. APPLICATIONS

A. Acoustic modes in a cell

Gillis *et al.* [18] calculated the acoustic eigenmodes for their experimental geometry, taking into account the growing a_w^{-1} and ζ. In the following, we will present a simpler version in a one-dimensional cell, $0 < x < L$, taking into account these two ingredients. In this case ω is treated as one of the eigenvalues and is complex, while we have assumed $\omega > 0$ in the previous section. Then ω should have a positive imaginary part for the stability of the system. Here $\sqrt{i\omega} = (1+i)\sqrt{\omega/2}$ for $\omega > 0$, while $\sqrt{i\omega} = (1-i)\sqrt{|\omega|/2}$ for $\omega < 0$. The latter follows from the requirement that the real part of κ in Eq.(2.17) should be positive. For general complex ω, all the quantities introduced so far should be functions of ω analytic for $\mathrm{Re}(i\omega) > 0$ or for $\mathrm{Im}\omega < 0$. Therefore, $X_\pm(-\omega) = X_\pm(\omega^*)^*$ and

$$Z(-\omega^*) = Z(\omega)^*, \quad W(-\omega^*) = W(\omega)^*, \quad (3.1)$$

where ω^* is the complex conjugate of ω.

Under the boundary conditions (2.28) and (2.30), the interior density deviation is expressed as

$$\delta\rho = \alpha(e^{ikx} + Ze^{-ikx}), = \alpha'(e^{ik(L-x)} + Ze^{-ik(L-x)}), \quad (3.2)$$

in terms of $Z = \beta/\alpha$. The first and second lines follow from Eqs.(2.28) and (2.30), respectively, and should coincide so that $\alpha' e^{ikL} = \beta$ and $\alpha' Z e^{-ikL} = \alpha$, leading to $Ze^{-ikL} = Z^{-1}e^{ikL}$. We now find the condition of the eigenmodes,

$$Z = \pm e^{ikL}, \quad (3.3)$$

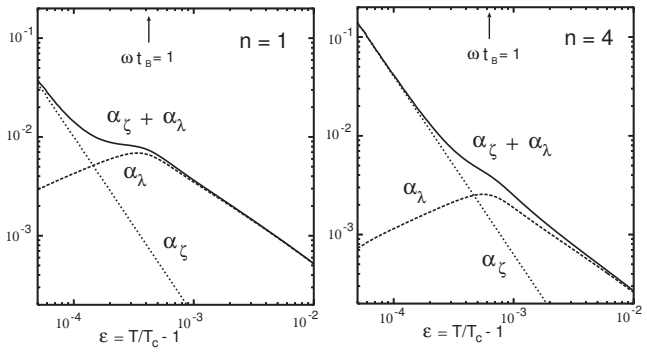

FIG. 3: Normalized damping constants α_λ, α_ζ, and $\alpha_\lambda + \alpha_\zeta$ defined by (3.5) and (3.6) vs $\epsilon = T/T_c - 1$ for $n = 1$ (left) and $n = 4$ (right). The resonant frequencies are close to $\omega = n\pi c/L \sim n \times 4 \times 10^4 \mathrm{sec}^{-1}$, which are exceeded by t_B^{-1} close to the critical point as marked by the arrows.

where + corresponds to even modes and − to odd modes. Namely, the density and temperature deviations are even (odd) functions of $x - L/2$ for the the even (odd) modes. For $W = (1-Z)/(1+Z)$ calculated in Eq.(2.32) or Eq.(2.40), we obtain

$$W = -i\tan(kL/2) \quad \text{(even modes)} = i\cot(kL/2) \quad \text{(odd modes)}. \quad (3.4)$$

Since W is small, the eigenfrequencies ω_n ($n = 1, 2, 3\cdots$) are nearly equal to $n\pi c^*/L$ where c^* is defined by Eq.(2.39). In the case $|W| \ll 1$ the leading correction from W can be written as

$$\omega_n = (n\pi + 2iW + \cdots)c^*/L, = [1 + i\alpha_\lambda + i\alpha_\zeta + \cdots]\mathrm{Re}\omega_n, \quad (3.5)$$

where $n = 2, 4, \cdots$ for the even modes and $n = 1, 3, \cdots$ for the odd modes. We assume small bulk damping $|\Delta_v| \ll 1$ and define

$$\alpha_\lambda = \frac{2}{n\pi}\mathrm{Re}W, \quad \alpha_\zeta = \frac{1}{2}|\Delta_v| = n\pi\frac{\zeta}{2\rho cL}, \quad (3.6)$$

where α_λ represents the boundary damping and α_ζ the bulk damping. The resonance quality factor Q^{-1} [18] is equal to $2(\alpha_\lambda + \alpha_\zeta)$ in our notation. The resonance frequency including the shift is given by the real part,

$$\mathrm{Re}\omega_n = (n\pi - 2\mathrm{Im}W + \cdots)\mathrm{Re}c^*/L. \quad (3.7)$$

The frequency ω in c^* and W may be equated with $\mathrm{Re}\omega_n \cong n\pi c/L$.

In Fig. 3, we show α_λ, α_ζ, and the sum $\alpha_\lambda + \alpha_\zeta$ as functions of ϵ in the regime $\omega t_\xi < 1$ for the odd mode of $n = 1$ and the even mode of $n = 4$ for CO_2 in a Cu cell with $L = 1$cm. We notice the following. (i) For such long wavelength sounds, the boundary damping is relevant far from the critical point, but the bulk damping eventually dominates close to the critical point. (ii) In accord with the discussion around Eq.(2.44), α_λ

decreases on approaching the criticality in the region of $t_B > \omega^{-1} \sim L/n\pi c$, with a maximum at $\omega t_B \sim 1$. As a result, the curve of the sum $\alpha_\lambda + \alpha_\zeta$ is flattened considerably around $t_B \sim \omega^{-1}$.

These theoretical results are consistent with the experimental data by Gillis *et al.*[18]. They performed the resonance experiment over a wide range of ωt_ξ (up to about 200) to measure the frequency-dependent bulk viscosity. In agreement with the theory [1, 3], α_ζ or $\omega\zeta/\rho c^2$ became independent of ϵ in the high-frequency regime $\omega t_\xi > 1$ (see Eq.(B5) in Appendix B).

B. Periodic perturbations

Periodic perturbations may be applied to a fluid in a cell in various manners. Resonance can occur when the frequency ω is close to $\mathrm{Re}\omega_n$. It is sharp for small $\mathrm{Im}\omega_n$. We will give three boundary conditions at $x = 0$ leading to resonance. We assume the boundary condition Eq.(2.30) at $x = L$. Then use of Eq.(3.2) yields $\alpha = \beta Z e^{-2ikL}$. The interior density deviation is of the form,

$$\delta\rho = \beta e^{-ikx} + \beta Z e^{ikx-2ikL}, \tag{3.8}$$

where the term proportional to Z arises from the reflection at $x = L$.

The bulk damping of the reflected waves is represented by $|e^{-ikL}| = e^{-\delta_B L}$. From Eq.(2.19) δ_B is expressed as

$$\delta_B = A_B(\omega/\pi c)^2, \tag{3.9}$$

in the low frequency regime $\omega t_\xi < 1$. We find $A_B = 0.5\times 10^{-3}$cm and 0.03cm at $\epsilon = 10^{-3}$ and 10^{-4}, respectively, for CO_2. In the relatively high frequency range $\omega > (2A_B)^{-1/2}\pi c/L$, the factor $e^{-2ikL}(\propto e^{-2\delta_B L})$ becomes negligibly small. Then, near the boundary, $\delta\rho$ consists of the outgoing wave only, resulting in no resonance. On the other hand, in the high frequency regime $\omega t_\xi > 1$, Eq.(B6) gives

$$\delta_B \cong \omega \mathrm{Im}\Delta_v/2c \cong 0.27\omega/\pi c, \tag{3.10}$$

which means that a sound emitted at $x = 0$ reaches the other end with the damping factor $e^{-0.27}$ for the first resonance frequency $\omega \cong \pi c/L$.

1. Temperature oscillation

In the first example, the temperature in the wall region $x < 0$ is oscillated, while the boundary walls are mechanically fixed. More precisely, we require $\delta T \to T_w \propto e^{i\omega t}$ as $x \to -\infty$; then, $\delta T(x) = e^{\kappa_w x}[\delta T(0) - T_w] + T_w$ in the region $x < 0$. The thermal boundary condition at $x = 0$ is then given by

$$\delta T' = a_w(i\omega/D)^{1/2}(\delta T - T_w), \tag{3.11}$$

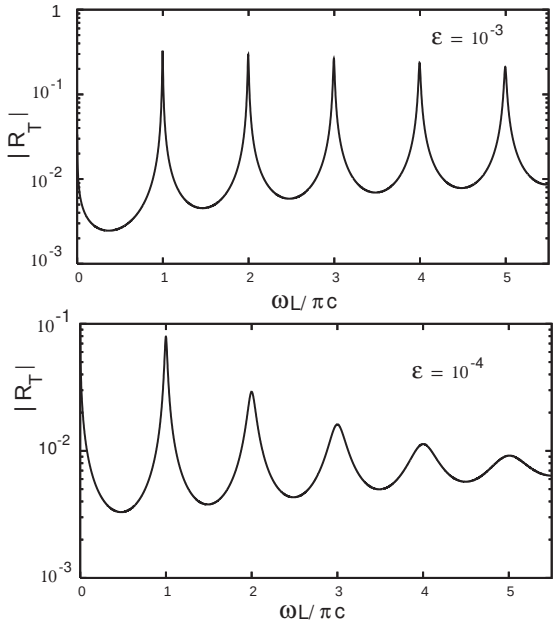

FIG. 4: Absolute value of the response function $R_T(\omega)$ in Eq.(3.12) vs $\omega L/\pi c$ on a semi-logarithmic scale for $\epsilon = 10^{-3}$ (upper panel) and 10^{-4} (lower panel) applicable for CO_2 in a Cu cell with $L = 1$ cm.

as a generalization of Eq.(2.28). Some calculations using Eqs.(2.23) and (2.25) give the response function defined by $R_T \equiv \beta/b_s T_w$ in the form,

$$R_T = \frac{1}{2}(1 + \gamma D k^2/i\omega)\frac{1 - Z}{1 - Z^2 e^{-2ikL}}. \tag{3.12}$$

Notice that R_T diverges as $R_T \cong cW/2iL(\omega - \omega_n)$ for $\omega = \omega_n$ $(n = 1, 2, \cdots)$ in the complex ω plane from Eq.(3.3). Under the adiabatic condition Eq.(2.34), the interior temperature deviation is expressed as

$$\delta T = b_s^{-1}\delta\rho = (e^{-ikx} + Z e^{ikx-2ikL})R_T T_w. \tag{3.13}$$

Furthermore, neglecting $\gamma D k^2/i\omega$ in Eq.(3.12) and using $|W| \ll 1$ (see Fig. 2), we obtain

$$R_T \cong W/[1 - (1 - 4W)e^{-2ikL}]. \tag{3.14}$$

In Fig. 4, we plot the absolute value $|R_T|$ calculated from Eq.(3.12) vs the normalized frequency $\omega L/\pi c$ at $\epsilon = 10^{-3}$ and 10^{-4}, using the data for CO_2 in a Cu cell with $L = 1$cm [20]. It exhibits peaks at $\omega \cong n\pi c/L$ as expected, but its peak heights do not exceeds 1/2 due to the small factor $1-Z \cong 2W$ in the numerator in Eq.(3.12) As discussed below Eq.(3.9), the resonant peaks should disappear for $\omega L/\pi c > (2A_B)^{-1/2}$, where we may neglect e^{-2ikL} in R_T to obtain $R_T \cong W$. These results are in accord with Fig. 4, since $(2A_B)^{-1/2} \cong$30 and 4 for $\epsilon = 10^{-3}$ and 10^{-4}, respectively.

In the low frequency case $\omega \ll c/L$, the interior deviations become nearly homogeneous. Figure 1 indicates that t_B can much exceed L/c very close to the critical

point, while $|\Delta_v| \ll 1$ holds. Thus, retaining $\gamma\Delta_v$, we set $e^{ikL} \cong 1 + ikL$ and $1 + \Delta_v \cong 1$ and use Eqs.(2.40) and Eq.(3.12) to find

$$R_T \cong \frac{1}{4}[\sqrt{i\omega t_1}X_v + 1]^{-1}, \tag{3.15}$$

where t_1 is defined by Eq.(1.1) and X_v by Eq.(2.41). If $\omega \ll t_B^{-1}$, we further have $R_T \cong (\sqrt{i\omega t_1'} + 1)^{-1}/4$ with

$$t_1' = (1 + a_w^{-1})^2 t_1 = (1 + a_w^{-1})^2 L^2/4(\gamma - 1)^2 D, \tag{3.16}$$

which is related to t_2 in Eq.(2.43) by $t_1' t_2 = L^2/4c^2$. The t_1' first decreases as $t_1 \sim \epsilon^{2.26}$ for $a_w \gg 1$ but finally weakly increases as $t_1 a_w^2 \cong \epsilon^{-0.22}$ for $a_w \ll 1$. See Fig. 1 for the curve of t_1'. As will be discussed in Subsection III C, t_1' is the piston time including the effect of the wall heat conduction [14].

We need to know when $|\sqrt{i\omega t_1}X_v| \gg 1$ holds. It holds for $\omega \gg 1/t_1'$ under the condition,

$$(1 + a_w^{-1})^{-2} t_B/t_1' = (1 + a_w^{-1})^{-4} t_B/t_1 \ll 1. \tag{3.17}$$

If $a_w < 1$ for CO_2 in a Cu cell, the above condition becomes $a_w^4 t_B/t_1 = 2 \times 10^{-6}\epsilon^{-0.97}/L^2 \ll 1$ with L in cm , which is well satisfied for $\epsilon \gg 10^{-6}$ with $L = 1$cm. If $\omega t_1' \ll 1$ under Eq.(3.17), we find

$$\delta T \cong T_w/2, \tag{3.18}$$

in the interior. Note that the reverse condition of Eq.(3.17), $a_w^4 t_B/t_1 > 1$, holds extremely close to the critical point, where $|\sqrt{i\omega t_1}X_v| > 1$ and $R_T \cong 1/4i\omega\sqrt{t_1 t_B}$ are obtained for $\omega \gg (t_1 t_B)^{-1/2}$. See the discussion below Eq.(3.32) for the relaxation behavior in this ultimate regime.

Zhong *et al.* [11] measured a density change induced by boundary temperature oscillation in near-critical ^{3}He, where the frequency was very low ($\omega/2\pi < 2$Hz) and the bulk viscosity was not important. However, they could measure in-phase and out-of-phase response in agreement with the original theory [3].

2. Mechanical oscillation

In the second example, the boundary wall at $x = 0$ is mechanically oscillated without heat input from outside. This is the case in the usual acoustic experiments using a piezoelectric transducer[18]. Let $u_w(\propto e^{i\omega t})$ be the applied displacement amplitude; then,

$$v = i\omega u_w \tag{3.19}$$

at $x = 0$ in Eq.(2.12). Assuming Eq.(2.30) and using Eq.(3.8) we obtain

$$\begin{aligned} \beta &= -\left[1 + \frac{\kappa}{a_w}\sqrt{\frac{D}{i\omega}}\right]\frac{\kappa R_T}{1 - \gamma D\kappa^2/i\omega}\rho u_w \\ &= (\gamma - 1)^{-1}\sqrt{i\omega/D}X_v R_T \rho u_w \end{aligned} \tag{3.20}$$

where the first line is general and the second line is the approximation under the adiabatic condition Eq.(2.34). Since the response is proportional to R_T, resonance occurs as in the previous case of temperature oscillation.

In the low frequency case $\omega \ll c/L$, the interior density change is nearly homogeneous and

$$\delta\rho \cong 2\beta \cong \left[1 - \frac{1}{\sqrt{i\omega t_1}X_v + 1}\right]\frac{\rho u_w}{L}, \tag{3.21}$$

which is the counterpart of Eq.(3.14). As discussed below Eq.Eq.(3.16), $\sqrt{i\omega t_1}X_v$ is large in the relatively high-frequency range $\omega \gg 1/t_1'$ under Eq.(3.17). Thus the interior density deviation behaves as

$$\begin{aligned} \delta\rho &\cong \rho u_w/L \quad (1/t_1' \ll \omega \ll c/L) \\ &\cong \sqrt{i\omega t_1}X_v \rho u_w/L \quad (\omega \ll 1/t_1'), \end{aligned} \tag{3.22}$$

under Eq.(3.17). The volume change mostly occurs in the bulk region for $1/t_1' \ll \omega \ll c/L$ and in the thermal diffusion layers for $\omega t_1' \ll 1$.

3. Heat flux oscillation

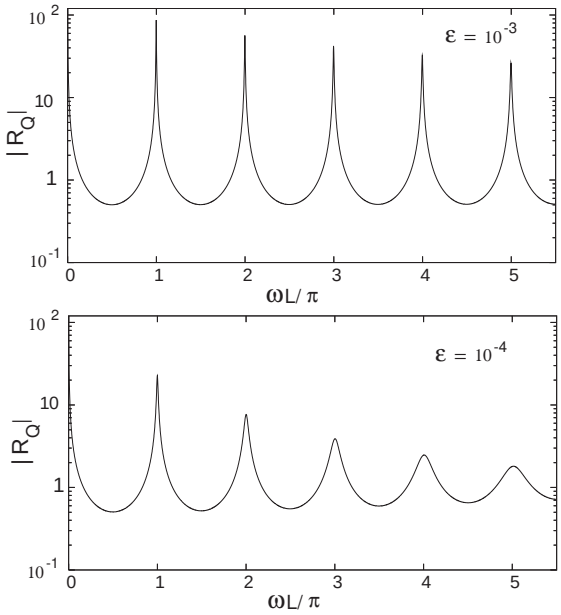

FIG. 5: Absolute value of the response function $R_Q(\omega)$ in Eq.(3.24) vs $\omega L/\pi c$ on a semi-logarithmic scale for $\epsilon = 10^{-3}$ (upper panel) and 10^{-4} (lower panel) applicable for CO_2 in a Cu cell with $L = 1$ cm.

In the third example, we apply a heat flux $\dot{Q}_0 = -\lambda(dT/dx)_{x=0} \propto e^{i\omega t}$ at $x = 0$ assuming the boundary condition (2.30). It is convenient to introduce a dimensionless response function R_Q by

$$\beta = \frac{\rho}{cT}\left(\frac{\partial T}{\partial p}\right)_s R_Q \dot{Q}_0 \tag{3.23}$$

Then Eqs.(2.26) and Eq.(3.8) give

$$R_Q = \frac{ick/D}{(1+\gamma\Delta_v)(k^2+\kappa^2)(1-Ze^{-2ikL})} = \frac{1}{(1+\Delta_v)^{3/2}(1-Ze^{-2ikL})}, \quad (3.24)$$

where the first line is general and the second line holds under the adiabatic condition (2.34). In the complex ω plane, R_Q has poles ω_n', which are equal to ω_{2n} in Eq.(3.5) with system length changed to $2L$. Thus R_Q grows for $\omega \cong n\pi c/L$ for $\omega < (2A_B)^{-1/2}\pi c/L$. In Fig. 5, we plot the absolute value $|R_Q|$ as a function of $\omega L/\pi c$ for $\epsilon = 10^{-3}$ and 10^{-4}. We can see that $|R_Q|$ is larger than $|R_T|$ in Fig. 4 roughly by two orders of magnitude.

The behavior of R_Q in the low frequency range $\omega \ll c/L$ is very different from that of R_T, however. From the second line of Eq.(3.24) we have $R_Q \cong 1/(2ikL+2W)$ to obtain the counterpart of Eq.(3.15),

$$R_Q \cong \frac{X_v}{2\sqrt{i\omega t_2}}[1+2\sqrt{i\omega t_1}X_v]^{-1}. \quad (3.25)$$

Under Eq.(3.17) we find that $R_Q \cong (1+a_w^{-1})/2\sqrt{i\omega t_2}$ for $\omega \ll 1/t_1'$ and $R_Q \cong 1/4i\omega\sqrt{t_1 t_2}$ for $1/t_1' \ll \omega \ll c/L$.

In this situation we may calculate the heat flux $\dot{Q}_L$ at $x = L$. From Eq.(2.26) it is written as

$$\dot{Q}_L = \frac{(1-Z)e^{-ikL}}{1-Ze^{-2ikL}}\dot{Q}_0, \quad (3.26)$$

which vanishes for $Z = 1$ (or for $a_w = 0$) and becomes small with increasing $\delta_B L$. Near the resonance frequency $n\pi c/L$, the ratio $\dot{Q}_L/\dot{Q}_0$ behaves as $(-1)^n W/[i(\omega L/c - n\pi) + n\pi\zeta/2\rho c^2 + W]$. The low frequency behavior for $\omega \ll c/L$ is given by

$$\dot{Q}_L = (1+2\sqrt{i\omega t_1}X_v)^{-1}\dot{Q}_0. \quad (3.27)$$

From the discussion below Eq.(3.16), we find $\dot{Q}_L \cong \dot{Q}_0$ for $\omega t_1' \ll 1$ under Eq.(3.17). That is, an applied heat flux passes through a near-critical fluid on the time scale of t_1' under Eq.(3.17), due to the piston effect.

C. Thermal and mechanical piston effects

1. Boundary temperature change

In the original papers of the piston effect [3], the boundary temperatures at $x = 0$ and L were both raised by a common small amount T_1 at $t = 0$. Subsequently, the boundary temperatures were held fixed for $t > 0$. In this paper, we examine the effects of finite a_w^{-1} [14, 18] and large ζ [16, 17]. We suppose that the system was in equilibrium for $t < 0$ and the temperature in the wall region $x < 0$ was instantaneously raised by T_1 at $t = 0$ without external heat input in the other wall region $x > L$. The boundary conditions are then given by

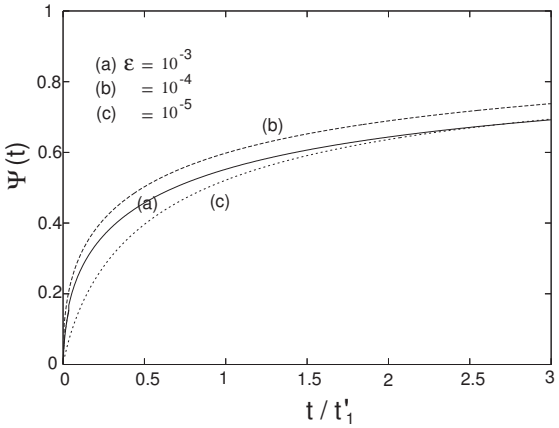

FIG. 6: Relaxation function $\Psi(t)$ in Eq.(3.29) defined by Eq.(3.30) vs t/t_1' at $\epsilon = 10^{-3}$, 10^{-4}, and 10^{-5} for CO_2 in a Cu cell with $L = 1$ cm, which is applicable for $t \gg L/c$. The time t_1' is defined in Eq.(3.16). Functional form of $\Psi(t)$ as a function of t/t_1' is rather insensitive to ϵ since Eq.(3.17) holds for this case.

$\delta T(x,t) \to T_1$ as $x \to -\infty$ and $\delta T(x,t) \to 0$ as $x - L \to \infty$ for $t > 0$. All the deviations vanish for $t < 0$.

The Fourier transformation of the interior temperature deviation $\delta T(x,t)$ with respect to t is given by Eq.(3.13) with $T_w = T_1 e^{i\omega t}/i\omega$ (since $\int_0^\infty dt e^{-i\omega t} = 1/i\omega$). The inverse Fourier transformation gives

$$\frac{\delta T(x,t)}{T_1} = \int \frac{d\omega e^{i\omega t}}{2\pi i\omega}(e^{-ikx} + Ze^{ikx-2ikL})R_T, \quad (3.28)$$

where the integration is in the range $[-\infty, \infty]$. Under Eq.(2.34), $W = W(\omega)$ and $R_T = R_T(\omega)$ are given by Eqs.(2.40) and (3.12), respectively. The integrand is analytic (without singularities) in the lower half plane $\mathrm{Im}\omega < 0$ and hence the integral is nonvanishing only for $t > 0$.

In the time region $t \gg L/c$ we may neglect the space dependence of $\delta T(x,t)$ in the interior and use the simple expression (3.15) for $R_T(t)$. It then follows

$$\delta T(t) = T_1\Psi(t)/2, \quad (3.29)$$

where we introduce the dimensionless relaxation function $\Psi(t)$. Its Fourier transformation reads

$$\int_0^\infty dt e^{-i\omega t}\Psi(t) = \frac{1}{i\omega(\sqrt{i\omega t_1}X_v + 1)}. \quad (3.30)$$

The inverse Fourier transformation of the right hand side of Eq.(3.30) may be transformed into an integral along the positive imaginary axis $\mathrm{Im}\omega > 0$. With X_v being defined by Eq.(2.41), we generally find $\Psi(t) > 0$ for $t > 0$, $\Psi(t) \cong t/\sqrt{t_1 t_B}$ as $t \to 0$, and $\Psi(t) = 1 - (t_1'/\pi t)^{1/2} + \cdots$ as $t \to \infty$. In particular, not very close to the critical point, we may neglect the bulk viscosity and take the limit $t_B \to 0$; then, $X_v \to 1 + a_w^{-1}$ and $\Psi(t) \to \Psi_0(s)$,

where $\Psi_0(s)$ is a universal function of $s = t/t_1'$ expressed as [3]

$$\Psi_0(s) = 1 - \int_0^\infty \frac{du}{\pi\sqrt{u}} \frac{e^{-us}}{1+u} = 1 - e^s \mathrm{erfc}(\sqrt{s}), \quad (3.31)$$

where erfc $= 1 -$ erc is the complementary error function and $\Psi_0 \cong 2(s/\pi)^{1/2}$ for $s \ll 1$ and $\Psi_0 \cong 1 - 2(\pi s)^{-1/2}$ for $s \gg 1$.

In Fig. 6, we display $\Psi(t)$ as a function of t/t_1' at $\epsilon = 10^{-3}$, 10^{-4}, and 10^{-5} for CO_2 in a Cu cell with $L = 1$ cm. For $\epsilon = 10^{-3}$ we can see $\Psi(t) \cong \Psi_0(t/t_1')$, where $t_B/t_1' \sim 0.02$ from Table 1. The discussion below Eq.(3.16) indicates that $\Psi(t)$ approaches unity on the time scale of t_1' as long as Eq.(3.17) is satisfied. This is the case even for $\epsilon = 10^{-5}$, where $t_B/t_1' \cong 21$ from Table 1. In fact, if $t_B/t_1' \gg 1$ and $a_w \ll 1$, we may set $\sqrt{i\omega t_1}X_v \cong i\omega\sqrt{t_1 t_B} + a_w^{-1}\sqrt{i\omega t_1}$, where the second term is relevant in $\Psi(t)$ under Eq.(3.17), again leading to $\Psi(t) \cong \Psi_0(t/t_1')$ for $t > a_w^2 t_B$. However, the reverse condition of Eq.(3.17) holds extremely close to the critical point, where $R_T \cong 1/[i\omega\sqrt{t_1 t_B} + 1]$ holds yielding [17]

$$\Psi(t) \cong 1 - \exp(-t/\sqrt{t_1 t_B}). \quad (3.32)$$

The new relaxation time $\sqrt{t_1 t_B}$ here grows as $\sqrt{t_1 t_B} \cong 1.0 \times 10^{-4} L\epsilon^{-0.64}$sec for near-critical CO_2.

Assuming the isothermal boundary ($a_w = \infty$), Carlès and Dadzie examined the bulk viscosity effect in the thermal equilibration [17]. Their relaxation function is obtained if we set $X_v = (1 + i\omega t_B)^{1/2}$ in Eq.(3.30). Then a new viscous regime appears for $t_1 \gg t_B$ with $\Psi(t)$ being given by Eq.(3.32), while the usual piston regime is encountered for $t_1 \ll t_B$. For CO_2 we have $t_B/t_1 \cong 2.7 \times 10^{-20} L^{-2}\epsilon^{-4.63}$, so $t_1 = t_B$ holds at $\epsilon \cong 0.6 \times 10^{-4}$ with $L = 1$cm. In our calculations based on Eq.(3.17), the different predictions have arisen from the reduced temperature dependence of a_w or the crossover of the boundary condition into the insulating one.

2. *Volume change*

We suppose a volume change by moving the boundary wall at $x = 0$ by a small length u_1 instantaneously at $t = 0$ [1]. We assume the thermal boundary conditions (2.28) and (2.30) at $x = 0$ and L. As in Eq.(3.26), the complete interior density deviation is the inverse Fourier transformation of Eq.(3.8), where β is given by Eq.(3.20) with $u_w = u_1 e^{i\omega t}/i\omega$.

Here we are interested in the late stage $t \gg L/c$, where the interior deviations depend only on t. The inverse Fourier transformation of Eq.(3.21) gives the interior deviations,

$$\delta\rho(t) = b_s \delta T(t) = [1 - \Psi(t)]\rho u_1/L, \quad (3.33)$$

where $\Psi(t)$ defined by Eq.(3.30) represents the effect of the thermal diffusion layers at $x = 0$ and L. The above form with $\Psi = \Psi_0$ was derived in Ref.[1]. If $u_1 > 0$, the interior is adiabatically heated by $b_s^{-1}\rho u_1/L$ on the acoustic time scale L/c after the volume change, while the boundary wall temperature is almost unchanged. Subsequently, the thermal diffusion layers become effective as *reverse* pistons and the interior temperature deviation decays as $(t_1'/t)^{1/2}$.

The reverse piston effect itself generally occurs on the time scale of t_1' after a near-critical fluid was adiabatically heated or cooled. Miura *et al.* observed such a process after a pulse-like heat input (see Fig. 2 in Ref.[20]).

D. Emission of sound

We examine sound emission at the boundary at $x = 0$. We neglect the incoming wave reflected at the other end $x = L$ and consider the semi-infinite limit $L \to \infty$.

The problem is simple in the case of boundary wall motion. An emitted sound propagates with the velocity c and integration of the continuity equation gives the density deviation,

$$\delta\rho(x,t) \cong \rho v_1(t - x/c)/c, \quad (3.34)$$

where $v_1(t)$ is the velocity of the boundary. The localized part of the density deviation (the term proportional to a in Eq.(2.20)) should be small when differentiated with respect to time. In fact, under the adiabatic condition (2.34), Eqs.(3.12) and (3.20) lead to

$$\beta \cong \frac{1+Z}{2(1+\Delta_v)c} i\omega\rho u_w, \quad (3.35)$$

for $e^{-2ikL} \to 0$. If we set $1 + \Delta_v \cong 1$ and $Z \cong 1$, the above relation becomes $\beta \cong i\omega\rho u_w/c$, leading to Eq.(3.34). Here $i\omega u_w$ is the Fourier transformation of $v_1(t)$ multiplied by $e^{i\omega t}$. Thus Eq.(3.34) holds on time scales longer than t_ξ (even when the time scale of $v_1(t)$ is shorter than t_B).

A sound is also emitted when a time-dependent heat flux $\dot{Q}_0(t)$ is supplied at the boundary at $x = 0$. From Eq.(3.8) the Fourier transformation of the interior density deviation $\delta\rho(x,t)$ is of the form βe^{ikx} with β being given by Eq.(3.23). Under the adiabatic condition Eq.(2.34) we may use the second line of Eq.(3.24) to find the convolution relation,

$$\delta\rho(x,t) = \frac{\rho}{cT}\left(\frac{\partial T}{\partial p}\right)_s \int_{-\infty}^t d\tau \Phi(x, t-\tau)\dot{Q}_0(\tau). \quad (3.36)$$

The memory function $\Phi(x,t)$ is defined for $t > 0$ as

$$\Phi(x,t) = \int \frac{d\omega}{2\pi} e^{i\omega t - ikx}(1+\Delta_v)^{-3/2}, \quad (3.37)$$

where $\Delta_v = i\omega\zeta/\rho c^2 = i\omega R_B t_\xi$ with $R_B \cong 0.03$. The time integration of this function is normalized as $\int_0^\infty dt\Phi(x,t) = 1$. From the integration in the region

$\omega < t_\xi^{-1}$ we obtain the long-time behavior $\Phi(0,t) \cong (4t/\pi t_\zeta^3)^{1/2} e^{-t/t_\zeta}$ with $t_\zeta \equiv R_B t_\xi$ at $x = 0$. Since this relaxation is rapid, we may set $\Phi(0,t) \cong \delta(t)$ (δ-function) at $x = 0$ on time scales longer than t_ξ or when $\dot{Q}_0(t)$ varies slower than t_ξ. Furthermore, if the distance x is not large such that the bulk damping is negligible in the region $0 < x < L$, we may set $\Phi(x,t) \cong \delta(t - x/c)$ to find the simple formula for the emitted sound,

$$\delta\rho(x,t) = \frac{\rho}{cT}\left(\frac{\partial T}{\partial p}\right)_s \dot{Q}_0(t - x/c), \tag{3.38}$$

as the counterpart of Eq.(3.34). On the other hand, use of Eq.(B6) for Δ_v gives the short-time behavior,

$$\Phi(0,t) = (\hat{\alpha}/2\hat{\nu})(t/t_\xi)^{\hat{\alpha}/2\hat{\nu}}/t, \tag{3.39}$$

valid in the time region $t \lesssim t_\xi$ with $\hat{\alpha}/2\hat{\nu} \cong 0.088$ (see Appendix B). This behavior is detectable only for an increase of $\dot{Q}_0$ within a time shorter than t_ξ.

Miura *et al.* applied a stepwise heat flux with $\dot{Q}_0 = 0.183 \times 10^7$ to find a stepwise outgoing sound with $\delta\rho/\rho \cong 2.2 \times 10^{-7}$ for CO_2, where $\dot{Q}_0$ is in cgs units (erg/cm^{2}sec) [20]. Our theoretical expression (3.38) becomes $\delta\rho/\rho = 1.38 \times 10^{-13} \dot{Q}_0$ with the aid of $(\partial T/\partial p)_s \cong T_c/6.98 p_c$ for CO_2 [35]. For their experimental $\dot{Q}_0$ our theory gives $\delta\rho/\rho = 2.55 \times 10^{-7}$ in fair agreement with the observed density change. Furthermore, they could generate sound pulses with duration of order 10μsec by applying short-time heat input. They were interested in the adiabatically increased energy $E_{\rm ad} \equiv p \int dx \delta\rho(x,t)/\rho$ in the pulse region per unit area. Here Eq.(3.38) yields [3]

$$E_{\rm ad} = \frac{p}{T}\left(\frac{\partial T}{\partial p}\right)_s Q, \tag{3.40}$$

where $Q = \int dt \dot{Q}_0(t)$ is the total heat supplied. The ratio $E_{\rm ad}/Q$ represents the efficiency of transforming applied heat to mechanical work. Theoretically, it is given by $(\partial T/\partial p)_s p/T$ as in Eq.(3.40) and is equal to $1/6.98 = 0.14$ for near-critical CO_2 [35]. The measured values of the ratio $E_{\rm ad}/Q$ were in the range $0.11 - 0.12$ again in fair agreement with our theory.

E. Reflection of sound

Reflection of plane wave sounds is discussed for an isothermal boundary in the textbook of Landau-Lifshitz [34]. Miura *et al.* [20] observed reflected pulses passing through a detector in the cell. Their shapes gradually flattened after many traversals within the cell, resulting in the interior temperature homogenization. At present, it is not clear how to understand their data. Here, as a first step, we will derive some fundamental relations on sound reflection.

We consider a pulse approaching to the boundary at $x = 0$ in the semi-infinite limit $L \to \infty$. Reflection takes place upon its encounter with the wall. The density deviations of the incoming and outgoing pulses are obtained as the inverse Fourier transformation of Eq.(2.20). Neglecting the bulk damping in the neighborhood of the boundary, we may express them as $\rho_i(t + x/c)$ and $\rho_o(t - x/c)$, respectively. Using $\alpha(\omega) = e^{i\omega t} \int d\tau e^{-i\omega\tau} \rho_i(\tau)$ and $\beta = Z\alpha$, we obtain

$$\rho_o(t) = \int \frac{d\omega}{2\pi} \int dt' Z(\omega) e^{i\omega(t-t')} \rho_i(t'). \tag{3.41}$$

The interior density deviation is the sum $\delta\rho(x,t) = \rho_i(t + x/c) + \rho_o(t - x/c)$. Since $Z(0) = 1$, the excess mass is invariant upon reflection as

$$\Delta M = \int dt \rho_i(t) = \int dt \rho_o(t). \tag{3.42}$$

This relation holds if we integrate a long tail of the reflected pulse $\rho_o(t)$ at large t (see Eq.(3.47)).

If $\rho_i(t)$ changes much slower than t_ξ, we may set $Z \cong 1 - 2W$ with $W = (\gamma - 1)\sqrt{i\Delta_T}/X_v$ from Eq.(2.40). In this approximation we may rewrite Eq.(3.40) in the following convolution form,

$$\begin{aligned} \rho_o(t) &= \rho_i(t) - \int_0^\infty d\tau \dot{\chi}(\tau)[\rho_i(t-\tau) - \rho_i(t)] \\ &= \rho_i(t) - \int_0^\infty d\tau \chi(\tau) \dot{\rho}_i(t-\tau) \end{aligned} \tag{3.43}$$

where $\dot{\chi}(t) = \partial\chi(t)/\partial t$ and $\dot{\rho}_i(t) = \partial\rho_i(t)/\partial t$. From Eq.(3.41) the function $\chi(t)$ is the inverse Fourier transformation of $(1 - Z)/i\omega \cong 2W/i\omega$. Some calculations (in the complex ω plane) give $\chi(t)$ in the integral form,

$$\chi(t) = \varepsilon_r \int_0^\infty \frac{d\Omega}{\pi\sqrt{\Omega}} {\rm Re}\left[\frac{e^{-\Omega s}}{a_w^{-1} + \sqrt{1 - \Omega}}\right], \tag{3.44}$$

where $s = t/t_B$ is the scaled time, ${\rm Re}[\cdots]$ denotes taking the real part, and $\sqrt{1 - \Omega} = i\sqrt{\Omega - 1}$ for $\Omega > 1$. The dimensionless parameter ε_r is defined by

$$\varepsilon_r = 2(\gamma - 1)\sqrt{D/c^2 t_B} \tag{3.45}$$

which decreases near the critical point as $\varepsilon_r \cong 4.3\epsilon^{0.75}$ for CO_2. The function $\chi(t)$ depends only on s and a_w. For $a_w \gg 1$ we have $\chi(t)/\varepsilon_r \cong e^{-s/2} I_0(s/2)$ with I_0 being the modified Bessel function, while for $a_w \ll 1$ we have $\chi(t)/\varepsilon_r \cong 1 - \Phi_0(s/a_w^2)$ with Φ_0 being defined in Eq.(3.31). Thus $\chi(t)$ changes on the scale of $t_B' \equiv t_B(1 + a_w^{-1})^{-2}$ and its limiting behaviors are as follows:

$$\begin{aligned} \frac{\chi(t)}{\varepsilon_r} &= (1 + a_w^{-1})^{-1} (\pi s)^{-1/2} + \cdots \quad (s \to \infty), \\ &= 1 - 2a_w^{-1} (s/\pi)^{1/2} + \cdots \quad (s \to 0). \end{aligned} \tag{3.46}$$

In addition, the second term of Eq.(3.43) representing the distortion is negative (positive) when $\rho_i(t)$ is increasing (decreasing). This initial drop is because of heating and expansion of the pulse at the boundary.

From the first line we obtain $\dot{\chi}(t) \cong -(t_2/\pi)^{1/2}t^{-3/2}$ for $t \gg t'_B$. (i) Let $\rho_i(t)$ is peaked in the region $|t| < t_0$; then, for $t \gg t'_B$ and t_0, the first line of Eq.(3.43) gives a long-time tail of the reflected wave,

$$[\rho(t)]_{\rm tail} = \Delta M(t_2/\pi)^{1/2}t^{-3/2} \tag{3.47}$$

where ΔM is defined by Eq.(3.42). If $t_0 > t'_B$, the total mass behind the peak is given by the time integral of the tail Eq.(3.47) in the region $[t_0, \infty]$. Thus the mass fraction behind the peak is $(4t_2/\pi t_0)^{1/2}$. For CO_2 this quantity is estimated as $10^{-7}\epsilon^{-0.75}t_0^{-1/2}$ with t_0 in sec for $a_w \gg 1$. (ii) As another example, we consider a stepwise change, where $\rho_i(t)$ is equal to 0 for $t < 0$ and to a constant ρ_1 for $t > t_0$ with t_0 being the transient time. Then, for $t \gg t'_B$ and t_0, the second line of Eq.(3.43) gives a longer tail,

$$[\rho(t)]_{\rm tail} = \rho_1(4t_2/\pi)^{1/2}t^{-1/2}. \tag{3.48}$$

The bulk viscosity does not appear in these tails.

When $\rho_i(t)$ changes much slower than t'_B, only the long time behavior of $\chi(t)$ is relevant in $\rho_o(t)$. From Eq.(3.43) we find the following convolution relations,

$$\begin{aligned}\rho_o(t) &= \rho_i(t) + \sqrt{\frac{t_2}{\pi}}\int_0^\infty \frac{d\tau}{\tau^{3/2}}[\rho_i(t-\tau) - \rho_i(t)] \\ &= \rho_i(t) - \sqrt{\frac{4t_2}{\pi}}\int_0^\infty \frac{d\tau}{\sqrt{\tau}}\dot{\rho}_i(t-\tau),\end{aligned} \tag{3.49}$$

from which the long-time tails (3.47) and (3.48) readily follow. The above expressions contain only t_2 in Eq.(2.43) and not t_B. They are widely applicable far from the critical point (where t_B becomes short). With decreasing ϵ for the isothermal boundary ($a_w > 1$), t_2 grows and the distortion of the reflected pulse increases as long as the pulse width is longer than t_B. However, if the pulse width is shorter than t'_B, the distortion decreases on approaching the critical point since ε_r in Eq.(3.45) decreases.

As a simple illustration, let us consider a Gaussian pulse $\rho_i(t) = \rho_1 \exp(-t^2/2t_0^2)$, where ρ_1 is the pulse height and t_0 is the pulse width. Since its Fourier transformation is $(2\pi)^{1/2}\rho_1 t_0 e^{-\omega^2 t_0^2/2}$, we may readily calculate $\rho_o(t)$. In Fig. 7, we plot the normalized pulse deformation defined by

$$F_G(t) = [\rho_o(t) - \rho_i(t)]/(\rho_1\sqrt{t_2/t_0}). \tag{3.50}$$

The curve (a) is for the limiting case $t_B/t_0 \to 0$ and $a_w = \infty$, while $t_B/t_0 = 10$ and $a_w = 0.63$ in (b), and $t_B/t_0 = 50$ and $a_w = 0.63$ in (c). In Table 1 we have $a_w = 0.63$ and $t_B = 1.9$msec at $\epsilon = 10^{-4}$ for CO_2 in a Cu cell, where pulses with $t_0 \ll t_B$ are well possible [20]. We recognize that the distortion is negative for $t \lesssim t_0$ and is positive for $t \gtrsim t_0$ (in accord with the comment below Eq.(3.43)) and that the distortion is decreased as t_B/t_0 is increased or for shorter pulses due to the bulk viscosity growth.

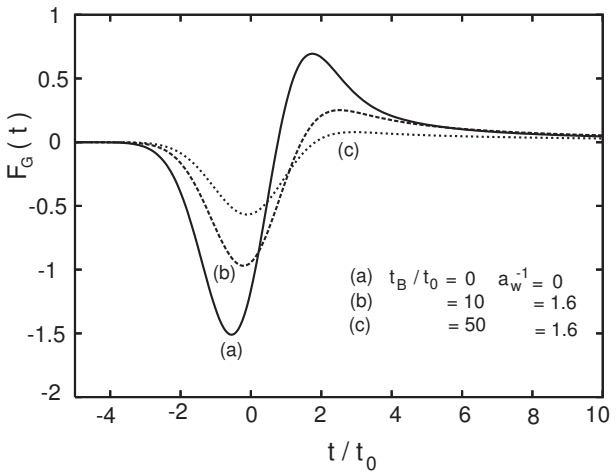

FIG. 7: Scaled pulse deformation $F_G(t)$ defined by Eq.(3.50) vs scaled time t/t_0 for a Gaussian incoming pulse with width t_0 for $t_B/t_0 \to 0$ and $a_w = \infty$ (a), $t_B/t_0 = 10$ and $a_w = 0.63$ (b), and $t_B/t_0 = 50$ and $a_w = 0.63$ (c).

IV. SUMMARY AND REMARKS

In summary, we have examined various thermoacoustic effects in one-component supercritical fluids in a one-dimensional geometry. We summarize our main results.

(i) In the linear hydrodynamics, sound modes and thermal diffusion modes are both present as in Eq.(2.20), depending on given boundary conditions. The latter modes can be absent only for the insulating boundary condition $a_w = 0$. The calculations are straightforward and the final expressions are much simplified under the adiabatic condition (2.34) or for low frequencies $\omega \ll c^2/\gamma D$. It is remarkable that the bulk viscosity ζ appears in the combination $\omega\gamma\zeta/\rho c^2 = \omega t_B$ as first pointed out by Carlès [16, 17]. The resultant characteristic time t_B grows as $\epsilon^{-3.0}$, while the life time of the critical fluctuations t_ξ grows as $\epsilon^{-1.9}$.

(ii) We have introduced the reflection factor $Z(\omega)$ as the ratio between outgoing and incoming sounds. Using Z or $W = (1-Z)/(1+Z)$ we have examined the acoustic eigenmodes, the response of the fluid to applied oscillation of the boundary temperature, the boundary heat flux, and the boundary position. To these thermal and mechanical perturbations, resonance is induced when the frequency of the perturbation is close to one of the eigenfrequencies, while nearly uniform adiabatic changes are caused in the interior at much lower frequencies owing to the piston effect.

(iii) We have also examned the response to a stepwise change of the boundary temperature and the boundary position. The relaxation time is given by the modified piston time t'_1 in Eq.(3.16) first introduced by Ferrell and Hao [14]. It is equal to the original piston time t_1 in Eq.(1.1) for the isothermal boundary $a_w \gg 1$ and to

$a_w^{-2}t_1$ for the insulating boundary $a_w \ll 1$.
(iv) As the critical point is approached, the role of the thermal diffusion layers is eventually diminished both by decreasing of the effusivity ratio a_w and by growing of the bulk viscosity ζ, while the bulk sound attenuation becomes increasing stronger. The bulk viscosity effect in the thermal diffusion layer is thus masked by its enhanced effect in the bulk.
(v) For CO_2 in a Cu cell, the boundary becomes thermally insulating for $\epsilon \ll 10^{-4}$. This suppresses the bulk viscosity effect in the thermal diffusion layers as long as Eq.(3.17) holds or for $\epsilon > 10^{-6}$. In this case, the viscous regime predicted by Carlès and Dadzie emerges for $\epsilon < 10^{-6}$ [16, 17]. To increase this crossover reduced temperature, the cell length L needs to be shorter. For the wall materials in Ref.[18], this crossover occurs much closer to the critical point [15].
(vi) We have also examined sound emission and reflection at the boundary, which are elementary hydrodynamic processes but seem to have not been well examined [34]. For emission, the formulas (3.34) and (3.38) are valid for a mechanical piston and a thermal heat input on time scales longer than t_ξ. For reflection, Eq.(3.43) with Eq.(3.44) holds on time scales longer than t_ξ. The formula (3.49) is the classical one valid on time scales much longer than t_B, where the distortion of the outgoing pulse increases on approaching the critical point. For pulses shorter than t_B, the distortion of the outgoing pulse is decreased as can be seen in Fig. 7.

In this paper, we have treated near-critical fluids in one phase states. However, more challenging are hydrodynamic effects in in two phase states, where latent heat transport, wetting dynamics, and Marangoni convection come into play in addition to the piston effect [36, 37, 38].

Acknowledgments

I would like to thank the members of the experimental group of the piston effect in Japan [20], Takeo Satoh, and P. Carlès for valuable discussions. Thanks are also due to Horst Meyer, K.A. Gillis, and M.R. Moldover for informative correspondence. This work was supported by grants from the Japan Space Forum and from the 21st Century COE project (Center for Diversity and Universality in Physics) from the Ministry of Education, Culture, Sports, Science and Technology of Japan.

Appendix A: Simple theory of the piston effect

Here we give a simple derivation of t_1 in Eq.(1.1). Let us apply a small heat δQ to a fluid from the boundary per unit area in the one dimensional geometry. The volume expansion of the thermal diffusion layers is given by $(\partial T/\partial p)_s A\delta Q(t)/T$, where A is the area of the heater surface and use is made of the Maxwell relation $(\partial \rho^{-1}/\partial s)_p = (\partial T/\partial p)_s$. The interior density change and the pressure change δp are nearly homogeneous in the interior and are given by

$$\delta\rho = \frac{\delta p}{c^2} = \frac{\rho}{T}\left(\frac{\partial T}{\partial p}\right)_s \frac{\delta Q}{L}. \tag{A1}$$

where $L = V/A$ is the cell length. The interior temperature deviation is caused adiabatically as $\delta T = (\partial T/\partial p)_s \delta p$ and is written as

$$\delta T = (\gamma - 1)\delta Q/C_p L, \tag{A2}$$

where $C_p = \rho T(\partial s/\partial T)_p$ is the isobaric specific heat and use is made of Eq.(2.9). If the boundary temperature is raised by T_1 at $t = 0$, we have $\delta Q \sim C_p \ell(t) T_1$ in the early stage, where $\ell(t) = \sqrt{Dt}$ is the thickness of the thermal diffusion layer. If we set $\delta T = T_1/2$, Eq.(1.1) is reproduced.

The relation (A1) also follows from our formula Eq.(3.38). Let the heat input rate $\dot{Q}(t)$ from the boundary to the fluid change slowly compared to the acoustic time $t_a = L/c$. We suppose a time interval with width $\delta t \gg t_a$, in which $\dot{Q}(t)$ is almost unchanged. Since $\delta t/t_a$ is the traversal number much larger than unity, the adiabatic pressure and density increases in the interior region are given by

$$\delta\rho = \frac{\delta p}{c^2} = \frac{\delta t}{t_a}\frac{\rho}{cT}\left(\frac{\partial T}{\partial p}\right)_s \dot{Q}, \tag{A3}$$

as a result of superposition of many steps. In terms of the incremental heat supply $\delta Q = \dot{Q}\delta t$ we reproduce Eq.(A1).

Appendix B: Summary of critical behavior

Let a one-component fluid be on the critical isochore ($\rho = \rho_c$) with small positive $\epsilon = T/T_c - 1$ near the gas-liquid critical point. The physical parameters used in the table 1 and the figures are given below. Hereafter $\hat{\nu}(\cong 0.63)$, $\hat{\gamma}(\cong 1.24)$, and $\hat{\alpha}(\cong 0.10)$ are the usual critical exponents. Data of near-critical CO_2 can be found in Refs.[30, 35].

Our hydrodynamic description is valid when the spatial scale under investigation is longer than the correlation length $\xi = \xi_0 \epsilon^{-\hat{\nu}}$, where $\xi_0 = 1.5$Å for CO_2. The constant-volume specific heat $C_V = \rho T(\partial s/\partial T)_\rho$ and the isobaric specific heat $C_p = \rho T(\partial s/\partial T)_p$ are expressed as

$$C_V = A_V[\epsilon^{-\hat{\alpha}} + B], \quad C_p = A_p \epsilon^{-\hat{\gamma}}. \tag{B1}$$

For CO_2 on the critical isochore, the coefficients are given by $A_V = 26.3 k_B n^*$, $B = 0.9$, and $A_p = 2.58 k_B n^*$, where $n^* = p_c/k_B T_c \cong 1.76\times 10^{21}\mathrm{cm}^{-3}$. The specific-heat ratio γ grows strongly as $\gamma_0 \epsilon^{-\hat{\gamma}+\hat{\alpha}}$ if the background ($\propto B$) is neglected, where $\gamma_0 = 0.1$ for CO_2. The sound velocity and the constant-volume specific heat are weakly singular as $c^2 \propto \epsilon^{\hat{\alpha}}$ (if the background is neglected [1]). We have set $c = 2.3 \times 10^4 \epsilon^{0.06}$ cm sec^{-1} for CO_2 [20].

The thermal conductivity λ grows such that the thermal diffusion constant D behaves as

$$D = \lambda/C_p = k_B T/6\pi\eta\xi = D_0\epsilon^{\hat{\nu}}, \tag{B2}$$

where $D_0 = 4.0\times10^{-4}\mathrm{cm}^2\mathrm{sec}^{-1}$ for CO_2. Thus $\lambda \propto \epsilon^{\hat{\nu}-\hat{\gamma}}$. The relaxation time of the critical fluctuations with size ξ increases as

$$t_\xi = \xi^2/D = t_0\epsilon^{-3\hat{\nu}}, \tag{B3}$$

where $t_0 = 0.56\times10^{-12}$sec for CO_2. The shear viscosity η is only weakly singular and may be treated as a constant independent of ϵ and ω to make rough estimates. However, the zero-frequency bulk viscosity ζ grows very strongly as

$$\zeta = \rho c^2 R_B t_\xi, \tag{B4}$$

where R_B is a universal number estimated to be about 0.03 [1, 32]. For CO_2, $\zeta/\rho \cong 0.9\times10^{-5}\epsilon^{-2+2\hat{\alpha}}\mathrm{cm}^2\mathrm{sec}^{-1}$, so $\zeta/\rho D = \Delta_v/\Delta_T \cong 0.02\epsilon^{-2-\hat{\nu}+2\hat{\alpha}}$ (see Eqs.(3.13) and (3.14)). In the high frequency regime $\omega t_\xi \gg 1$, the complex sound velocity in Eq.(2.39) becomes asymptotically independent of ϵ [31, 32, 33]. Thus,

$$c^*(\omega) \cong c(i\omega t_\xi)^{\hat{\alpha}/6\hat{\nu}}. \tag{B5}$$

Since the exponent $\hat{\alpha}/6\hat{\nu}$ is small, we may set $\Delta_v = i\omega\zeta/\rho c^2 \cong (\hat{\alpha}/3\hat{\nu})\ln(i\omega t_\xi)$. Thus, in this high frequency regime, $\mathrm{Im}\Delta_v$ tends to the following universal number,

$$\mathrm{Im}\Delta_v = \pi\hat{\alpha}/6\hat{\nu} \cong 0.27\times 2/\pi \tag{B6}$$

In the high frequency regime $\omega t_\xi > 1$, Δ_v remains to be as a small quantity and the frequency-dependent bulk viscosity defined by $\zeta(\omega) \equiv \rho c^2\Delta_v/i\omega$ decays roughly as $1/i\omega$ with increasing ω.

Furthermore, in our thermoacoustic problems, we have introduced the time t_B in Eq.(2.37), which behaves as

$$t_B = t_B^0\epsilon^{-3\hat{\nu}-\hat{\gamma}+\hat{\alpha}}, \tag{B7}$$

where $t_B^0 = 1.7\times10^{-15}$sec for CO_2. The effusivity ratio a_w in Eq.(2.29) decreases as

$$a_w = a_w^0\epsilon^{\hat{\gamma}-\hat{\nu}/2}. \tag{B8}$$

For $a_w^0 \gg 1$ the boundary wall crosses over from an isothermal one to an thermally insulating one on approaching the critical point. For example, between Cu and CO_2, we have $a_w^0 = 3\times10^3$ [20], where $a_w < 1$ is reached for $\epsilon < 1.6\times10^{-4}$. The a_w^0 was smaller for the walls used in Ref.[15, 18].

[1] A. Onuki, *Phase Transition Dynamics* (Cambridge University Press, Cambridge, 2002).

[2] K. Nitsche and J. Straub, Proc. 6th European Symp. on Material Science under Microgravity Conditions (Bordeaux, France, 2-5 December 1986); J. Straub and L. Eicher, Phys. Rev. Lett. **75**, 1554 (1995).

[3] A. Onuki, H. Hao, and R. A. Ferrell, Phys. Rev. A **41**, 2256 (1990); A. Onuki and R.A. Ferrell, Physica A **164**, 245 (1990).

[4] H. Boukari, J.N. Shaumeyer, M.E. Briggs, and R.W. Gammon, Phys. Rev. A **41**, 2260 (1990) ; Phys. Rev. Lett. **65**, 2654(1990).

[5] R.A. Wilkinson, G.A. Zimmerli, H. Hao, M.R. Moldover, R.F. Berg, W.L. Johnson, R.A. Ferrell and R.W. Gammon, Phys. Rev. E **57**, 436 (1998).

[6] B. Zappoli, D. Bailly, Y. Garrabos, B. Le Neindre, P. Guenoun and D. Beysens, Phys. Rev. A **41**, 2264 (1990); P. Guenoun, B. Khalil, D. Beysens, Y. Garrabos, F. Kammoun, B. Le Neindre, and B. Zappoli, Phys. Rev. E **47**, 1531 (1993); Y. Garrabos, M. Bonetti, D. Beysens, F. Perrot, T. Fröhlich, P. Carlès and B. Zappoli, Phys. Rev. E **57**, 5665 (1998).

[7] R.P. Behringer, A. Onuki and H. Meyer, J. Low Temp. Phys. **81**, 71 (1990).

[8] H. Klein, G. Schmitz and D. Woermann, Phys. Rev. A **43**, 4562 (1991).

[9] J. Straub, L. Eicher and A. Haupt, Phys. Rev. E **51**, 5556 (1995); J. Straub and L. Eicher, Phys. Rev. Lett. **75**, 1554 (1995).

[10] F. Zhong and H. Meyer Phys. Rev. E **51**, 3223 (1995); A. Kogan and H. Meyer, J. Low Temp. Phys. **112**, 419 (1998).

[11] F. Zhong, A. Kogan and H. Meyer, J. Low Temp. Phys. **108**, 161 (1997).

[12] B. Zappoli and A.D. Daubin, Phys. Fluids, **6**, 1929 (1995); D. Bailly and B. Zappoli, Phys. Rev. E **62**, 2353 (2000).

[13] T. Maekawa, K. Ishii, M. Ohnishi and S. Yoshihara, Adv. Space Res. **29**, 589 (2002); J. Phys. A, **37**, 7955 (2004).

[14] R.A. Ferrell and H. Hao, Physica A **197**, 23 (1993).

[15] The effusivity is defined by $\epsilon_f = (C\lambda)^{1/2} = CD^{1/2}$ for each material, where C is the isobaric specific heat per unit volume, λ is the thermal conductivity, and $D = \lambda/C$ is the thermal diffusivity. For Cu used in [20], $\epsilon_f/k_B = 2.6\times10^{23}\mathrm{cm}^{-2}\mathrm{sec}^{-1/2}$. In Ref.[18], $\epsilon_f/k_B = 4.6\times10^{22}$ for a stainless steel resonator and $\epsilon_f/k_B = 2.7\times10^{21}$ for a polymer-coated resonator in the same units. The diffusivity ratio is defined as in Eq.(2.29) in this paper.

[16] P. Carlès, Phys. Fluids, **10**, 2164 (1998).

[17] P. Carlès and K. Dadzie, Phys. Rev. E **71**, 066310 (2005).

[18] K.A. Gillis, I.I. Shinder, and M.R. Moldover, Phys. Rev. E **70**, 021201 (2004); **72**, 051201 (2005); K. A. Gillis, I. I. Shinder, and M. R. Moldover, Phys. Rev. Lett. **97**, 104502 (2006). In these papers they defined $\Delta_v = \omega\nu_\ell/c^2$ and $\Delta_T = \omega D/c^2$ without i.

[19] M. Ohnishi, S. Yoshihara, M. Sakurai, Y. Miura, M. Ishikawa, H. Kobayashi, T. Takenouchi, J. Kawai, K. Honda, and M. Matsumoto, Microgravity. Sci. Tech. XVI-1,306 (2005).

[20] Y. Miura, S. Yoshihara, M. Ohnishi, K. Honda, M. Matsumoto, J. Kawai, M. Ishikawa, H. Kobayashi, and A. Onuki, Phys. Rev. E **74**, 010101 (R) (2006).

[21] P. Carlès, Phys. Fluids **18**, 126102 (2006).
[22] A.B. Kogan, D. Murphy and H. Meyer, Phys. Rev. Lett. **82**, 4635 (1999); A.B. Kogan and H. Meyer, Phys. Rev. E **63**, 056310 (2001).
[23] H. Azuma, S. Yoshihara, M. Onishi, K. Ishii, S. Masuda, and T. Maekawa, Int. J. of Heat and Mass Transfer **42**, 771 (1999).
[24] T. Fröhlich, D. Beysens, and Y. Garrabos Phys. Rev. E **74**, 046307 (2006).
[25] S. Amiroudine, , P. Bontoux, P. Larroud, B. Gilly and B. Zappoli, J. Fluid Mech. **442**, 119 (2001).
[26] Y. Chiwata and A. Onuki, Phys. Rev. Lett. **87**, 144301 (2001); A. Furukawa and A. Onuki, Phys. Rev. E **66**, 016302 (2002).
[27] S.Amiroudine and B. Zappoli, Phys. Rev. Lett. 90, 105303 (2003); G. Accary, I. Raspo, P. Bontoux, and B. Zappoli, Phys. Rev. E **72**, 035301(R) (2005).
[28] E.B. Soboleva, Phys. Rev. E **68**, 042201 (2003).
[29] G. Accary, I. Raspo, P. Bontoux, and B. Zappoli, C.R. Mecanique, **332**, 209 (2004).
[30] H.L. Swinney and D.L. Henry, Phys. Rev. A **6**, 2586 (1973).
[31] R.A. Ferrell and J.K. Bhattacharjee, Phys. Lett. A **86**, 109 (1981); Phys. Rev. A **24**, R1643 (1981); Phys. Rev. A **31**, 1788 (1985).
[32] A. Onuki, Phys. Rev. E **55**, 403 (1997).
[33] R. Folk and G. Moser, Phys. Rev. E **57**, 683 (1998); ibid. **57**, 705 (1998).
[34] L.D. Landau and E.M. Lifshitz, *Fluid Mechanics* (Pergamon, 1959).
[35] P.C. Hohenberg and M. Barmartz, Phys. Rev. A **6**, 289 (1972).
[36] J. Hegseth, A. Oprisan, Y. Garrabos, V. S. Nikolayev, C. Lecoutre-Chabot, and D. Beysens Phys. Rev. E **72**, 031602 (2005).
[37] R. Wunenburger, Y. Garrabos, C. Lecoutre, D. Beysens, J. Hegseth, F. Zhong, and M. Barmatz, Int. J of Thermophysics **23**, 103 (2002).
[38] A. Onuki, Phys. Rev. E **75**, 036304 (2007).